89

Elliot Mandel, Physics Undergraduate Honors Thesis, supervised by Alexander S. Silbergleit, June 2000.

Precise Trapped Flux Signal Analysis in Gravity Probe B Experiment

Ilya Mandel

emandel@cs.stanford.edu

June 26, 2000

Abstract

Magnetic fluxons trapped on the superconducting gyroscopes used in the Gravity Probe B (GP-B) experiment produce an additional flux measured by the superconducting quantum interference device (SQUID). A better understanding of the signal caused by the trapped flux can lead to improvements in the quality of the GP-B data analysis. In this thesis, a spectral representation of the trapped flux signal is determined and exact expressions for the amplitudes of the spin minus roll harmonics are obtained. Some applications of these results to data analysis are discussed.

1 Introduction

Gravity Probe B (GP-B) is an experimental test of Einstein's general theory of relativity. The GP-B satellite, which will be launched late in 2001, will contain four gyroscopes. According to the predictions of general relativity, the angular momentum vectors of these gyroscopes should precess over the course of a year by 6.6 arcseconds in the plane of the orbit and by 42 milliarcseconds perpendicular to the plane of the circular orbit of 650 km altitude. In order to determine the direction of angular momentum of a gyroscope, its surface will be covered with a niobium coating, so that at the experimental temperatures (2.5K) the rotors will be superconducting and will thus develop a London moment [1]. The magnitude of this London moment is proportional to the rotor spin frequency and its direction coincides with that of the instantaneous angular velocity. The magnetic flux due to the London moment can be measured by the pick-up loop of the superconducting quantum interference device (SQUID) and is proportional to the small angle between the London moment vector and the pick-up loop plane, making it possible to measure this angle, i.e. providing the needed readout.

Since niobium is a type II superconductor [2], besides the desired London moment the superconducting rotor surface will also be pierced by lines of trapped magnetic flux (fluxons), creating paired quantum-sized sources of magnetic field of opposite sign (half-fluxons) attached to the surface. Magnetic fields caused by these fluxons will contribute to the total flux through the SQUID pick-up loop and will, therefore, affect the GP-B measurements. Thus it is rather important to accurately analyze the trapped flux contribution to the high frequency (HF) SQUID signal in order to minimize the

impact of trapped flux on the GP-B results.

Along with some difficulties in the data analysis, the trapped flux signal brings in some useful and potentially useful information. For instance, the spin and polhode frequencies are determined from it in the baseline GP-B analysis. Also, the variation of the even HF harmonics amplitudes can be used in principle as a back up for the London moment readout. This is another reason for trying to investigate the trapped flux more thoroughly.

The analysis of the trapped flux carried out so far [3, 4, 5] made possible the generation of a realistic trapped flux signal for the GP-B data reduction simulations [6]. The complicated time behavior of the signal depends, along with the rotor spin and polhode frequencies and satellite roll frequency, on the angle γ_B between the rotor symmetry axis and the angular momentum vector, the total number N of fluxons present, and the position of each half-fluxon on the rotor surface. Were all these parameters known for a given GP-B gyro, one could, in principle, calculate the trapped flux contribution and remove its low frequency (LF) part from the LF SQUID signal, thereby improving the accuracy of the experimental result. So far, in the baseline GP-B data analysis the spin and polhode frequency are determined from the HF telemetry data (the 6 lowest FFT harmonics of spin minus roll).

The aim of this thesis is to try to improve the analytical representation of the slowly varying amplitudes of HF harmonics. By doing this, we hope to provide new means for advanced trapped flux signal analysis, allowing one to determine some and, with luck, perhaps even all the parameters mentioned above.

Section 2 of the thesis contains a synopsis of earlier results on the trapped flux due to a stationary

half-fluxon and the half-fluxon kinematics due to gyroscope motion along with some elaborations. Section 3 presents a spectral analysis of the trapped flux signal. In particular, explicit expressions for the amplitudes of the harmonics of spin minus roll frequency are obtained in the limits valid for GP-B. In section 4 these amplitudes are related to the high frequency harmonics data that will be present in the GP-B telemetry. Methods of analysis of these data are discussed, and some preliminary results are given.

2 Expression for Trapped Flux through the Pick-up Loop

2.1 Trapped Flux of a Point Magnetic Charge as a Function of its Position

According to papers [4, 5], in which most of the results of this section are obtained, the magnetic field fluxons in the GP-B experiment may be considered as static and non-interacting ones. Therefore, the magnetostatic approach to calculating the flux can be used and, moreover, the total flux through the SQUID pick-up loop is the sum of the fluxes due to the individual fluxons. We may treat each half-fluxon as the point source of the magnetic field with coordinate angles ϑ_f, φ_f on the surface $r = r_g$ of the rotor, since the fluxon's size ($10^{-5}\,cm$ ([2], p. 184)) is much less than the size of the gyroscope (1.91 cm radius). Here, (r, ϑ, φ) describe the sperical coordinate system in which the origin coincides with the pick-up loop center and the z axis is perpendicular to the pick-up loop plane. The

dependence of the half-fluxon position angles ϑ_f, φ_f on time due to the rotation of the gyroscope will be discussed in section 2.2.

In these settings, the following formula for the magnetic flux of a single half-fluxon is obtained [3, 4]:

$$\Phi_f(\cos\vartheta_f) = \frac{\Phi_0}{2} F_\delta(\cos\vartheta_f);$$

$$F_\delta(s) = \sum_{k=0}^{\infty} (1-\delta)^{2k+1} P_{2k+1}(s) \left[P_{2k}(0) - P_{2k+2}(0)\right]$$

$$= \frac{2}{\sqrt{\pi}} \sum_{k=0}^{\infty} (-1)^k \frac{k+3/4}{(k+1)!} \Gamma(k+1/2)\, (1-\delta)^{2k+1} P_{2k+1}(s) \qquad (1)$$

Here δ is the dimensionless gap between the pick-up loop and the rotor, $0 \le \delta = (R - r_g)/R < 1$, where R is the pick-up loop radius and r_g is the gyroscope radius. The function $F_\delta(s)$ can be viewed as a transfer function that converts the "input" fluxon position signal $S_{in}(t) = \cos\vartheta_f(t)$ into the "output" trapped flux signal $S_{out}(t) = 0.5\Phi_0 F_\delta(S_{in}(t))$ that is present in the GP-B readout. It is physically obvious that $F_\delta(s)$ is an odd function of s; in particular, $F_\delta(0)$ is zero since there is no flux through the pick-up loop due to a half-fluxon located exactly in the plane of the loop. If the loop is located immediately on the surface of the gyroscope, the flux is obtained by setting $\delta = 0$ in (1), which then reduces to [3, 4, 5]:

$$F_0(s) = \frac{2}{\sqrt{\pi}} \sum_{k=0}^{\infty} (-1)^k \frac{k+3/4}{(k+1)!} \Gamma(k+1/2) P_{2k+1}(s) = \begin{cases} 1 & \text{if } 0 < s \le 1; \\ 0 & \text{if } s = 0; \\ -1 & \text{if } -1 \le s < 0. \end{cases} \qquad (2)$$

The physical interpretation of this formula is that, with the pick-up loop located on the gyroscope's surface, the flux remains constant while the half-fluxon stays in the same hemisphere of the rotor and

abruptly changes its sign when the half-fluxon crosses the plane of the loop. Expressions (1) and (2) are the main results of the Honors Thesis by L. Wai [3].

At the same time, equation (2) points out the problem with using formula (1) for the GP-B conditions, where $\delta = 0.025$ is rather close to zero. Although for any $\delta > 0$ the series (1) has an absolutely converging majorant, and, therefore, $F_\delta(s)$ is an analytical function of s, there is a jump discontinuity in the function at $s = 0$ when $\delta = 0$. Consequently, the convergence of series (1) deteriorates for small δ, thereby making this series useless for numerical calculations at small δ. As δ approaches zero, the transfer function approaches the Heavyside step function with a step at the origin (see fig. 1).

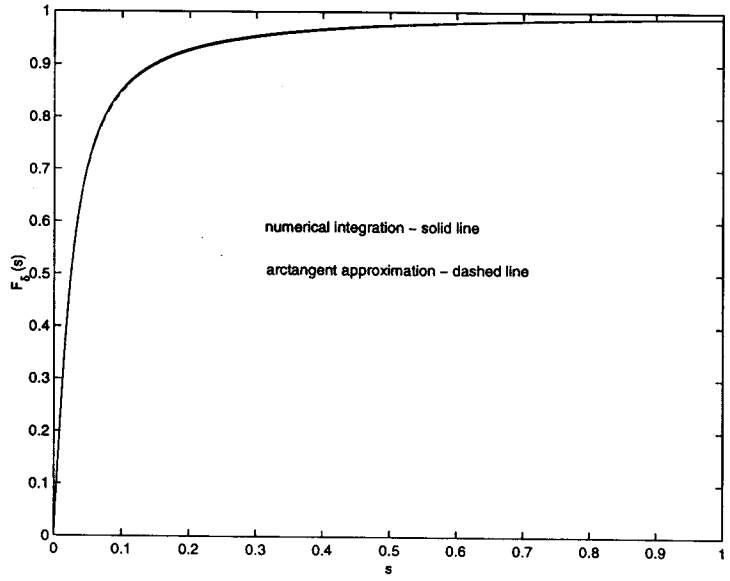

Fig. 1. Universal Curve $F_\delta(s)$ and Its Approximation.

One way to deal with the difficulties in the numerical calculation of $F_\delta(s)$ from expression (1) is

to use the integral representation of the trapped flux [5]:

$$F_\delta(\cos\vartheta_f) = \frac{\sqrt{2}}{\pi}\int_0^{\vartheta_f} \frac{d\psi \exp(i\psi/2)}{\sqrt{\cos\psi - \cos\vartheta_f}} \left[\frac{\lambda}{\sqrt{1+\lambda^2}} - \frac{\sqrt{1+\lambda^2}}{2\lambda} + \frac{1}{2\lambda}\right], \tag{3}$$

$$\lambda \equiv (1-\delta)\exp(i\psi)$$

Expression (3) may be conveniently used for computation because its integrand is algebraic and it is fairly easy to deal with the weak singularity at the upper limit.

Because of the described "kink" profile, the significant parameters of $F_\delta(s)$ for small δ are the value of its gradient at $s = 0$ and the "saturation" value $F_\delta(1)$. These quantities are calculated in [4, 5] to be:

$$f_\delta \equiv F_\delta(1) = \frac{1}{1-\delta}\left[1 - \frac{2\delta - \delta^2}{\sqrt{1+(1-\delta)^2}}\right] = 1 - (\sqrt{2}-1)\delta + O(\delta^2); \tag{4}$$

$$\kappa_\delta \equiv \left.\frac{\partial F_\delta(s)}{\partial s}\right|_{s=0} = \frac{2}{\pi(1-\delta)}\left[\frac{1+(1-\delta)^2}{1-(1-\delta)^2}\mathbf{E}(1-\delta) - \mathbf{K}(1-\delta)\right] = \frac{2}{\pi}\left[\frac{1}{\delta} + 2 + O(\delta\log\delta^{-1})\right], \tag{5}$$

where $\mathbf{K}(k)$, $\mathbf{E}(k)$ are complete elliptic integrals [8] of the first and second kind, respectively. A good approximation that has the correct slope at $s = 0$ and the correct value at $s = 1$ is the function

$$F_\delta(s) \approx A_\delta \arctan\frac{\kappa_\delta s}{A_\delta}, \qquad A_\delta \arctan\frac{\kappa_\delta}{A_\delta} = f_\delta, \qquad \delta \to +0 \tag{6}$$

The error of this approximation does not exceed 0.4% for $\delta = 0.025$. Moreover, equation (6) provides a very good approximation of the derivative: the error in the derivative does not exceed 1% in the region of interest ($s = O(\delta)$). The plots of both the exact expression (3) and its approximation (6) are given in fig. 1, and their respective derivatives are shown in fig. 2. For $\delta = 0.025$, we have $A_\delta \approx 0.637$.

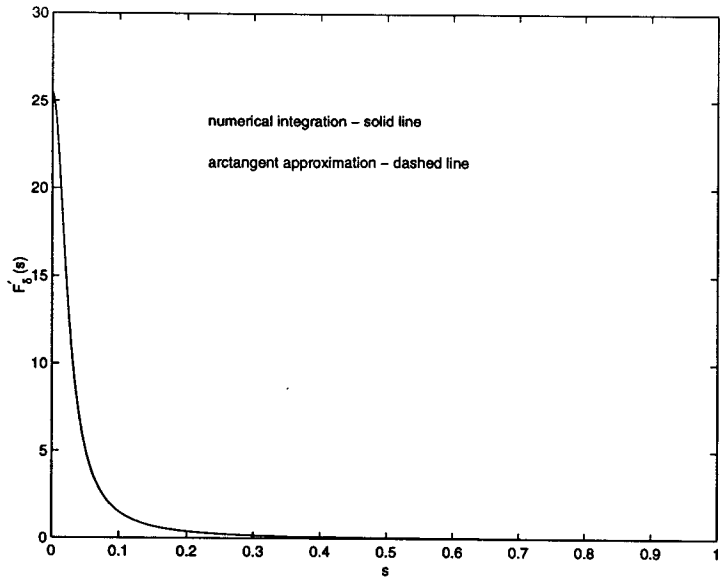

Fig. 2. Derivative $F'_\delta(s)$ and Its Approximation.

Although we have discussed the flux due to a single magnetic charge, our results can be easily applied to the GP-B situation in which $N \approx 100$ fluxons will be present on the gyroscope's surface after it is cooled below the transition temperature. By the principle of superposition, the total flux is simply the sum of the fluxes due to the individual half-fluxons. Therefore, if we denote the coordinate angles of half-fluxon i by $(\vartheta^i_\pm, \varphi^i_\pm)$, where '+' and '−' correspond to positive and negative half-fluxons, respectively, and i ranges from 1 to N, the total flux is:

$$\Phi(t) = \sum_{i=0}^{N} \Big[\Phi^i_+(t) + \Phi^i_-(t)\Big] = \frac{\Phi_0}{2} \sum_{i=0}^{N} \Big[F_\delta(\cos\vartheta^i_+(t)) - F_\delta(\cos\vartheta^i_-(t))\Big] \tag{7}$$

2.2 Kinematics of a Point Magnetic Charge

Before we can analyze the trapped flux signal we must determine the motion of the half-fluxon in space; in particular, we are interested in the behavior of $\vartheta_f(t)$, which is the angle between the vector in the direction of the half-fluxon on the rotor's surface and the normal to the pick-up loop.

First, note that the roll axis of the satellite can be regarded as fixed in inertial space since, besides a small poiniting error, the satellite always points at the Guide Star. Similarly, if we disregard torques (which are very small in the GP-B experiment) and the slow general relativistic drift, the angular momentum of the gyroscope, **L**, must remain fixed in inertial space. The roll axis lies almost exactly in the plane of the pick-up loop with a small misalignment $\alpha \leq 10^{-5}$ (see fig. 3) and **L** makes an angle $\beta \leq 10^{-5} rad$ with the satellite's roll axis (see fig. 4). Let us use the inertially fixed Cartesian coordinate system in which the **z** axis points along **L** and the **x** axis is perpendicular to both **L** and the satellite's roll axis. Then the normal to the pick-up loop can be written as:

$$\mathbf{n(t)} = \cos\alpha\cos(\theta_\mathbf{r})\mathbf{x} + (\cos\alpha\sin\theta_\mathbf{r}\cos\beta - \sin\alpha\sin\beta)\mathbf{y} + (\sin\alpha\cos\beta + \cos\alpha\sin\theta_\mathbf{r}\sin\beta)\mathbf{z}, \qquad (8)$$

where θ_r is the roll phase given by $\theta_r(t) = \omega_r t$.

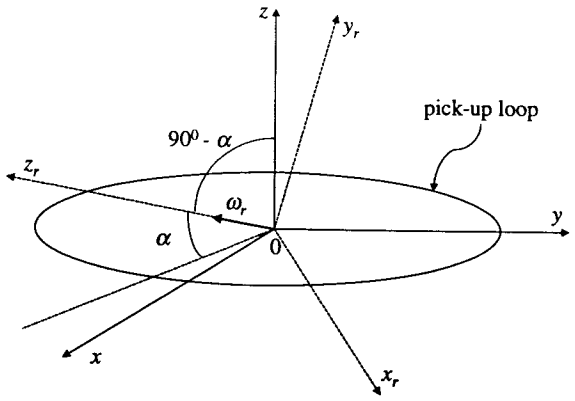

Fig. 3. Orientation of the roll axis with respect to the pick-up loop.

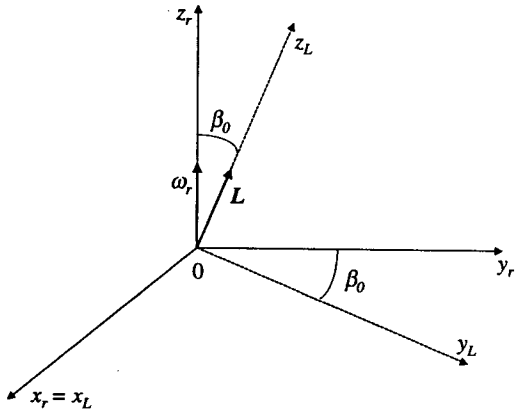

Fig. 4. Orientation of angular momentum with respect to the roll axis.

Next, we must determine the motion of the unit vector in the direction of the half-fluxon in the

same coordinate system. The GP-B rotors can be very accurately modeled by a symmetric top with the moments of inertia equal to $I + \delta I$ along the body symmetry axis and I along the other two principal axes. (A GP-B requirement states that $|\delta I|/I \leq 10^{-5}$.) The dynamics of the force-free motion of a symmetric top are well-known (see, for example, [9]). In particular, the spinning top's angular velocity is approximately $\omega_s = L/I$, while the angular velocity vector itself precesses around the body symmetry axis with angular frequency ([9], section 9)

$$\omega_p = \frac{L}{\delta I + I} \cos\gamma_B \frac{|\delta I|}{I} \approx \omega_s \frac{|\delta I|}{I} \cos\gamma_B, \tag{9}$$

where γ_B is the angle between the body symmetry axis and $\mathbf{z}$. If $\theta_s(t) = \omega_s t + \theta_s^0$ and $\theta_p(t) = \omega_p t + \theta_s^0$ denote the spin and polhode phases, respectively, we can transform the half-fluxon vector $\mathbf{e}$, corresponding to a half-fluxon located at (r_g, ξ, η) to our coordinates as follows:

$$\begin{aligned}
e_x(t) &= \sin\xi\,[\cos\gamma_B \cos\theta_s(t) \sin(\theta_p(t) + \eta) + \sin\theta_s(t) \cos(\theta_p(t) + \eta)] + \cos\xi \sin\gamma_B \cos\theta_s(t) \\
e_y(t) &= \sin\xi\,[\cos\gamma_B \sin\theta_s(t) \sin(\theta_p(t) + \eta) - \cos\theta_s(t) \cos(\theta_p(t) + \eta)] + \cos\xi \sin\gamma_B \sin\theta_s(t) \\
e_z(t) &= -\sin\xi \sin\gamma_B \sin(\theta_p(t) + \eta) + \cos\xi \cos\gamma_B
\end{aligned} \tag{10}$$

We can now compute the scalar product of $\mathbf{n(t)}$ and $\mathbf{e}$ to obtain the desired $\cos\vartheta_f(t)$. Making this computation to the first order in misalignments β and α we obtain, by means of equations (9) and (10) [5]:

$$\begin{aligned}
\cos\vartheta_f(t) &= \nu \sin\Theta + \epsilon(\beta \sin\theta_r + \alpha) \\
\Theta(t) &= (\omega_s - \omega_r)t + q; \qquad \theta_r(t) = \omega_r t + \theta_r^0
\end{aligned} \tag{11}$$

If the rotor is perfectly spherical, i.e. $\delta I = 0$, the ampltudes and initial phase $\nu = \sin\xi$, $q = \eta$ and $\epsilon = \cos\xi$ are all true constants. If, however, $\delta I \neq 0$, they vary slowly in time at the polhode frequency (9):

$$\nu(\omega_p t) = \sqrt{a^2 + b^2}, \qquad \tan q(\omega_p t) = \frac{b}{a}$$

$$\epsilon(\omega_p t) = \cos\gamma_B \cos\xi - \sin\gamma_B \sin\xi \sin(\omega_p t + \eta), \tag{12}$$

where

$$a = a(\omega_p t) = \cos\gamma_B \cos\xi + \sin\xi \cos(\omega_p t + \eta)$$

$$b = b(\omega_p t) = \cos\gamma_B \sin\xi \sin(\omega_p t + \eta)$$

The input to the the trapped flux tranfer function can therefore be described as a single harmonics of the spin minus roll frequency modulated in both phase and amplitude at the polhode frequency, with much smaller roll frequency and D.C. components that are also modulated at the polhode frequency.

A further study of the behavior of $\nu(\omega_p t)$ is necessary for the subsequent investigation. By definition, $\nu \geq 0$, but it is important to understand under what conditions it can actually turn to zero, and what its minimum value is when it does not. One should consider the following cases:

1. If $\cos\gamma_B = 0$, then $\nu(\omega_p t) = 0$ whenever $\cos(\omega_p t + \eta) = 0$. (If we were very lucky in the position of the half-fluxon, so that $\cos\xi = 0$, then ν is always zero and does not contribute to the signal at all.)

2. If $\cos\gamma_B \neq 0$, but $\tan\xi = \pm\cos\gamma_B$, then $\nu(\omega_p t) = 0$ whenever $\sin(\omega_p t + \eta) = 0$.

3. Finally, if the half-fluxon position and the angle γ_B are such that neither of these conditions hold, as will almost always be the case, $\nu(\omega_p t)$ can not equal zero. In fact, some trigonometric manipulation

shows that ν is bounded by:

$$\max \nu = \max \left[|\cos\gamma_B \cos\xi + \sin\xi|, |\cos\gamma_B \cos\xi - \sin\xi| \right]$$

$$\min \nu = \min \left[|\cos\gamma_B \cos\xi + \sin\xi|, |\cos\gamma_B \cos\xi - \sin\xi| \right]$$

These expressions are relevant to the discussion in section 3.3.

3 Spectral Representation of the Trapped Flux Signal

3.1 General Expression for the Amplitudes of Harmonics of Spin ± Roll

Let us now turn to the spectral analysis of the trapped flux signal transfer function, $F_\delta(\cos\vartheta_f(t))$. This is not entirely straightforward because $\cos\vartheta_f(t)$ is not a periodic function *of time*. However, by formula (11), it has the structure

$$\nu \sin\theta + \mu$$

with ν, θ and μ specified as functions of time by (11) and (12). Therefore $\cos\vartheta_f(t)$ and, with it, $F_\delta(\cos\vartheta_f(t))$, is a periodic function of θ, allowing for a Fourier expansion:

$$F_\delta(\nu\sin\theta + \mu) = \sum_{n=0}^{\infty} (\mathcal{A}_n \sin n\theta + \mathcal{B}_n \cos n\theta), \tag{13}$$

where

$$\mathcal{A}_n = \frac{1}{\pi}\int_{-\pi}^{\pi} F_\delta(\nu\sin\theta+\mu)\sin n\theta d\theta, \qquad \mathcal{B}_n = \frac{1}{\pi(1+\delta_{n0})}\int_{-\pi}^{\pi} F_\delta(\nu\sin\theta+\mu)\cos n\theta d\theta \tag{14}$$

Denoting the derivative of $F_\delta(s)$ in s by $F'_\delta(s)$ and integratng by parts in the expression (14) for $\mathcal{A}_n$ we obtain, using the fact that $F_\delta(s)$ is odd:

$$\mathcal{A}_n = \frac{1}{n\pi}\int_0^\pi \left[F'_\delta(\nu\sin\theta+\mu)+F'_\delta(\nu\sin\theta-\mu)\right]\nu\cos\theta\cos n\theta d\theta,$$
$$\mathcal{B}_n = \frac{1}{\pi(1+\delta_{n0})}\int_0^\pi \left[F_\delta(\nu\sin\theta+\mu)-F_\delta(\nu\sin\theta-\mu)\right]\cos n\theta d\theta \qquad (15)$$

Recall that in our analysis both the amplitude and the period vary slowly at the polhode frequency.

3.2 The Amplitudes of Harmonics in the Limit of Small μ

The smallness of the misalignments in GP-B guarantees that the second term of Eq. (11) is about 10^5 times smaller than the first. This allows us to consider $\cos\vartheta_f(t) = \nu\sin\theta+\mu$ in the limit $|\mu| \ll |\nu|$. Then, to the lowest order, equations (15) become:

$$\mathcal{A}_n = \frac{2}{n\pi}\int_0^\pi F'_\delta(\nu\sin\theta)\nu\cos\theta\cos n\theta d\theta + O\left(\mu^2\right),$$
$$\mathcal{B}_n = \frac{2\mu}{\pi(1+\delta_{n0})}\int_0^\pi F'_\delta(\nu\sin\theta)\cos n\theta d\theta + O\left(\mu^2\right) \qquad (16)$$

Since $F_\delta(s)$ is an odd function, $F'_\delta(s)$ is an even one. Therefore, the Taylor expansion of $F'_\delta(\nu\sin\theta)$ contains only even powers of $\nu\sin\theta$;

$$F'_\delta(\nu\sin\theta) = \sum_{j=0}^{\infty} K_j\nu^{2j}\sin^{2j}\theta$$

Substituting this into equations (16) and changing the order of summation and integration, we find:

$$\mathcal{A}_n = \frac{2\nu}{n\pi}\sum_{j=0}^{\infty}\left[K_j\nu^{2j}\int_0^\pi\left(\sin^{2j}\theta\cos\theta\cos n\theta d\theta\right)\right],$$

$$\mathcal{B}_n = \frac{2\mu}{\pi(1+\delta_{n0})} \sum_{j=0}^{\infty} \left[K_j \nu^{2j} \int_0^{\pi} \left(\sin^{2j}\theta \cos n\theta d\theta \right) \right] \tag{17}$$

Note that

$$\int_0^{\pi} \sin^{2j}\theta \cos n\theta d\theta = 0 \text{ for odd n,}$$

so

$$\int_0^{\pi} \sin^{2j}\theta \cos\theta \cos n\theta d\theta = \int_0^{\pi} \left[\sin^{2j}\theta \cos(n+1)\theta + \sin^{2j+1}\theta \sin n\theta d\theta \right] d\theta = 0 \text{ for even n}$$

(see [8], eq. 858.506). Hence the only nonvanishing $\mathcal{B}_n$ are those with even n and the only nonvanishing $\mathcal{A}_n$ are those with odd n. This allows us to rewrite equation (13) as follows:

$$F_\delta(\nu \sin\theta + \mu) = \sum_{k=0}^{\infty} \left[A_k \sin(2k+1)\theta + B_k \cos(2k\theta) \right], \tag{18}$$

where

$$A_k \equiv \mathcal{A}_{2k+1} = \frac{2\nu}{(2k+1)\pi} \int_0^{\pi} F'_\delta(\nu \sin\theta) \cos\theta \cos(2k+1)\theta d\theta,$$

$$B_k \equiv \mathcal{B}_{2k} = \frac{2\mu}{\pi(1+\delta_{k0})} \int_0^{\pi} F'_\delta(\nu \sin\theta) \cos 2k\theta d\theta \tag{19}$$

The same result was obtained in [4] by means of a different approach, which ensures the structure of (18) rather than (13) for the case of arbitary μ/ν.

3.3 Explicit Expression for the Harmonics Amplitudes

As mentioned previously, the transfer function $F_\delta(s)$ approaches a step function for small values of δ, which is the case in GP-B. Hence its derivative $F'_\delta(s)$ is proprotional to the Dirac delta function in

this limit. To determine the proportionality coefficient, we note that

$$\int_{-1}^{1} F'_\delta(s)ds = 2F_\delta(1)$$

Then,

$$F'_\delta(s) \approx 2F_\delta(1)\delta(s), \qquad \delta \to +0 \tag{20}$$

Now, by introducing $F'_\delta(s)$ from (20) into equations (19) for the harmonics amplitudes we obtain:

$$A_k \approx \frac{2\nu}{(2k+1)\pi}\int_0^\pi 2F_\delta(1)\delta(\nu\sin\theta)\cos\theta\cos(2k+1)\theta d\theta =$$

$$\frac{4\nu F_\delta(1)}{(2k+1)\pi}\int_0^\pi \frac{\delta(\sin\theta)}{\nu}\cos\theta\cos n\theta d\theta = \frac{4F_\delta(1)}{(2k+1)\pi} \tag{21}$$

$$B_k \approx \frac{2\mu}{\pi(1+\delta_{k0})}\int_0^\pi 2F_\delta(1)\delta(\nu\sin\theta)\cos 2k\theta d\theta = \frac{4\mu F_\delta(1)}{(1+\delta_{k0})\pi}\int_0^\pi \frac{\delta(\sin\theta)}{\nu}\cos 2k\theta d\theta = \frac{4\mu F_\delta(1)}{\nu(1+\delta_{k0})\pi}$$

The last step in the evaluation of both of the above integrals is based on the fact that the argument of the δ-function, $\sin\theta$, is equal to zero twice on the interval, at zero and π. However, since these two zeros are the two endpoints of the interval, the contribution due to each is half of the value of the integrand at that point.

In the integration above, we used the fact that for a non-zero m, $\delta(mx) = \delta(x)/m$. Unfortunately, as noted at the end of section 2.2, ν may come close to zero. Assuming that ν stays greater than the small parameter $\varepsilon = 2F_\delta(1)/\pi\kappa_\delta$, we can write down a more precise approximation, which at least gives a finite value for B_k whenever $\nu = 0$:

$$A_k \approx \frac{4F_\delta(1)}{(2k+1)\pi}\frac{2}{\pi}\arctan\frac{\nu}{\varepsilon} + O(\varepsilon^2)$$

$$B_k \approx \frac{4\mu F_\delta(1)}{\nu(1+\delta_{k0})\pi}\frac{2}{\pi}\arctan\frac{\nu}{\varepsilon} + O(\varepsilon^2) \tag{22}$$

To do this, one needs to use the technique of asymptotic evaluation of integrals with so-called δ-like kernels [[11], [12]]. Note that depending on the fluxon position angle ξ and on γ_B, $\nu(\omega_p t)$ could in some cases become smaller that ε and even turn to zero (see discussion at the end of section 2.2). Whenever this happens, both (21) and (22) become invalid; however, that happens, if at all, only over relatively small intervals of time $\approx \varepsilon T_p \approx 0.025 T_p$, where $T_p = 2\pi/\omega_p$ is the polhode period. In addition, with a realistic number of fluxons for GP-B ($N \approx 100$), the probability that ν goes to zero simultaneously for more than one half-fluxon is extremely small, and an individual contribution of a single half-fluxon is almost negligible.

One may be surprised to see that in equations (22), A_k falls rather slowly with increasing k, while B_k is independent of k altogether, suggesting that the corresponding series may not converge at all. However, one should bear in mind that the above expressions are valid only for a bounded set of n, i.e., only for the first several harmonics. This approximation is sufficient in the case of GP-B, where only the first three odd harmonics ($k = 0, 1, 2$) and the first three even harmonics ($k = 0, 1, 2$) will be considered. In general, it can be shown via integration by parts that $A_k \leq C_h/(2k+1)^h$ for an arbitrary power h; however, C_h grows exponentially with h. On the other hand, if we use (22) for larger and larger k, the difference between the exact and approximate values will also grow.

We are now finally in a position to obtain the desrired spectral representation for the total trapped flux. We begin by computing the amplitudes of the harmonics of flux due to a single half-fluxon by

susbtituting eq. (21) into eq. (18). The first odd harmonics of $\Phi(t)$ (in particular, $k = 1, 2, 3$) are:

$$[\Phi(t)]_{2k+1} = \frac{\Phi_0}{2} A_k \sin(2k+1)\Theta$$

$$= \frac{2\Phi_0 F_\delta(1)}{(2k+1)\pi} \{\sin[(2k+1)(\omega_s - \omega_r)t] \cos(2k+1)q + \cos[(2k+1)(\omega_s - \omega_r)t] \sin(2k+1)q\} \quad (23)$$

The first even harmonics of $\Phi(t)$ (in particular, $k = 0, 1, 2$) are:

$$[\Phi(t)]_{2k} = \frac{\Phi_0}{2} B_k \sin(2k\Theta)$$

$$= \frac{2\Phi_0 \mu F_\delta(1)}{\nu(1+\delta_{k0})\pi} \{\cos[2k(\omega_s - \omega_r)t] \cos 2kq - \sin[2k(\omega_s - \omega_r)t] \sin 2kq\} \quad (24)$$

Now, we can generalize this to the case of N fluxon pairs by means of equation (7):

$$[\Phi_T(t)]_{2k+1} = \frac{2\Phi_0 F_\delta(1)}{(2k+1)\pi} \times$$

$$\sum_{i=1}^{N} \Big\{ \sin[(2k+1)(\omega_s - \omega_r)t] \cos(2k+1)q_+^i - \sin[(2k+1)(\omega_s - \omega_r)t] \cos(2k+1)q_-^i +$$

$$+ \cos[(2k+1)(\omega_s - \omega_r)t] \sin(2k+1)q_+^i - \cos[(2k+1)(\omega_s - \omega_r)t] \sin(2k+1)q_-^i \Big\} \quad (25)$$

$$[\Phi_T(t)]_{2k} = \frac{2\Phi_0 F_\delta(1)}{(1+\delta_{k0})\pi} \sum_{i=1}^{N} \Big\{ \frac{\mu_+^i}{\nu_+^i} \cos[2k(\omega_s - \omega_r)t] \cos 2kq_+^i - \frac{\mu_-^i}{\nu_-^i} \cos[2k(\omega_s - \omega_r)t] \cos 2kq_-^i -$$

$$- \frac{\mu_+^i}{\nu_+^i} \sin[2k(\omega_s - \omega_r)t] \sin 2kq_+^i + \frac{\mu_-^i}{\nu_-^i} \sin[2k(\omega_s - \omega_r)t] \sin 2kq_-^i \Big\}, \quad (26)$$

where $\nu_\pm^i$, $\mu_\pm^i$ and $q_\pm^i$ are functions of $\omega_p t$ and the coordinate angles $\xi_\pm^i, \eta_\pm^i$ of the i'th half-fluxon given by eq. (11) and (12).

4 Signal Analysis

4.1 GP-B High Frequency Signal Description

For the purposes of signal modeling and analysis it is more convenient to express the total trapped flux in terms of harmonics of $(\omega_s - \omega_r)$ whose amplitudes are modulated by the polhode frequency. Therefore, we will rewrite equations (25) and (26) as

$$\frac{\Phi_T(t)\pi}{2\Phi_0 F_\delta(1)} = \sum_{k=0}^{\infty} [D_k(\omega_p t)\sin(2k+1)(\omega_s-\omega_r)t + E_k(\omega_p t)\cos(2k+1)(\omega_s-\omega_r)t] +$$

$$(\beta \sin\omega_r t + \alpha)\sum_{k=0}^{\infty}[U_k(\omega_p t)\cos 2k(\omega_s-\omega_r)t - V_k(\omega_p t)\sin 2k(\omega_s-\omega_r)t], \tag{27}$$

with

$$D_k(\omega_p t) = \frac{1}{2k+1}\sum_{i=1}^{N}\left[\cos(2k+1)q_+^i(\omega_p t) - \cos(2k+1)q_-^i(\omega_p t)\right];$$

$$E_k(\omega_p t) = \frac{1}{2k+1}\sum_{i=1}^{N}\left[\sin(2k+1)q_+^i(\omega_p t) - \sin(2k+1)q_-^i(\omega_p t)\right];$$

$$U_k(\omega_p t) = \frac{1}{1+\delta_{k0}}\sum_{i=1}^{N}\left[\frac{\epsilon_+^i(\omega_p t)}{\nu_+^i(\omega_p t)}\cos 2kq_+^i(\omega_p t) - \frac{\epsilon_-^i(\omega_p t)}{\nu_-^i(\omega_p t)}\cos 2kq_-^i(\omega_p t)\right];$$

$$V_k(\omega_p t) = \frac{1}{1+\delta_{k0}}\sum_{i=1}^{N}\left[\frac{\epsilon_+^i(\omega_p t)}{\nu_+^i(\omega_p t)}\sin 2kq_+^i(\omega_p t) - \frac{\epsilon_-^i(\omega_p t)}{\nu_-^i(\omega_p t)}\sin 2kq_-^i(\omega_p t)\right]. \tag{28}$$

Here $\nu_\pm^i(\omega_p t)$, $\epsilon_\pm^i(\omega_p t)$ and $q_\pm^i(\omega_p t)$ depend on the fluxon position angles $\xi_\pm^i, \eta_\pm^i$ according to eq. (12). As explained in the previous section, expressions (28) for the coefficients are the lowest order approximation for a bounded set of numbers k. In the course of the GP-B experiment, the telemetry will provide the first three odd harmonics ($k = 0, 1, 2$) and the first three even harmonics, counting

D.C. ($k = 0, 1, 2$) of the quantity $C_S\Phi_T(t)$ (volts), where C_S is the SQUID scale factor. So, the following signals are assumed to be known:

$$w_k(t) = CD_k(\omega_p t) + noise; \qquad x_k(t) = CE_k(\omega_p t) + noise;$$

$$y_k(t) = C(\beta \sin \omega_r t + \alpha)U_k(\omega_p t) + noise; \qquad z_k(t) = -C(\beta \sin \omega_r t + \alpha)V_k(\omega_p t) + noise, \tag{29}$$

for $k = 0, 1, 2$.

Here

$$C = C_S 2F_\delta(1)/\pi \ \ (\text{volts/units } \Phi_0) \tag{30}$$

is the adjusted SQUID scale factor.

The noise level is expected to be about the same for the odd and even harmonics. However, the amplitudes of the even harmonics signal is several orders of magnitude smaller. Moreover, the even harmonics signal will be known with less accuracy because it will be truncated to reduce the total GP-B telemetry volume. Fore these reasons, we shall for now stay away from the analysis of the even harmonics, even though they may provide useful information, and concentrate on the odd ones. For the odd harmonics, on the other hand, the signal-to-noise ratio is expected to be $\sim 10^5$ or better. Thus, the electronic noise is smaller than the error in our approximation of the harmonic amplitudes, so we may disregard the noise in the odd harmonics altogether for the purposes of our analysis, at least in the initial approach.

For the purposes of HF signal investigation, we assume that the spin frequency and polhode frequency are known from the baseline GP-B data analysis and an estimate of $\cos\gamma_B$ can be obtained

from these via eq. (9), while the roll frequency is known since it is a commanded parameter. We wish to obtain from this analysis the total number of fluxons N, a more precise estimate of γ_B, and, ideally, the fluxon position angles $(\xi_{\pm}^i, \eta_{\pm}^i)$. Furthermore, the scale factor C either can be treated as a known parameter (it can be determined from the LF analysis), or we may attempt to estimate it during the HF analysis as well.

4.2 Determination of the Number of Fluxons

The first useful application of the theoretical calculation of the harmonics amplitudes lies in our ability to easily obtain an estimate for the total number of fluxons. Let us consider the average of the magnitudes squared of w_0 and x_0 over the polhode period. According to (29), this can be expressed in terms of the harmonics amplitudes as:

$$\left\langle w_0^2 + x_0^2 \right\rangle_{polhode} \equiv \frac{1}{T_p} \int_{t_0}^{t_0+T_p} \left(w_0^2 + x_0^2 \right) dt = C^2 \left\langle D_0^2 + E_0^2 \right\rangle_{polhode}$$

By (28), the sum $D_0^2 + E_0^2$ consists of two parts,

$$\sum_{i=1}^{N} \left[\cos^2 q_+^i(\omega_p t) + \cos^2 q_-^i(\omega_p t) + \sin^2 q_+^i(\omega_p t) + \sin^2 q_-^i(\omega_p t) \right] = \sum_{i=1}^{N} [1+1] = 2N,$$

and the sum of the crossterms $\cos q_{\pm}^i(\omega_p t) \cos q_{\pm}^j(\omega_p t)$ and $\sin q_{\pm}^i(\omega_p t) \sin q_{\pm}^j(\omega_p t)$ for $i \neq j$. Since the fluxon positions, and thus the phases $q_{\pm}^i$, are more or less random, it is natural to expect that these crossterms should average out to zero over the polhode period. Consequently, we find that

$$\left\langle w_0^2 + x_0^2 \right\rangle_{polhode} \approx 2NC^2 \tag{31}$$

Since we can determine the polhode period and the SQUID scale factor C by other means, this gives us a method for obtaining the number of fluxons on a gyroscope.

To verify this method, we took a sample GP-B SQUID high frequency harmonics signal that was generated earlier for the GP-B data reduction simulation. That signal included one hundred fluxons ($N = 100$), of which 60 were randomly distributed over the sphere, while the remaining 40 were placed quasi-randomly in such a way that they provided a net flux in the direction of the London moment. After performing the averaging operation via a Matlab program that was based on Simpson's integration method, we obtained a value of 226 for N from eq. (31). Although this is a considerable error, a significant portion of it can be attributed to the not completely random distribution of fluxons. In particular, if a sizeable fraction of the half-fluxons are arranged in such a way that the values of $\cos q$ are approximately equal for them, as was the case for 40 of the fluxons in the distribution we analyzed, the crossterms discussed above should not be expected to average out to zero over the polhode period, and their contribution will increase our estimate of N.

We should note here that in the lab experiments with the cooled rotors the fluxon number was estimated by the maximum value of the trapped flux through the pick-up loop divided by Φ_0. This generally yields values that are a factor of 2 lower than the true number of fluxons because fluxons are not lined up and thus do not yield their maximum contributions to the total flux at the same instance of time; the result of this approach for the signal studied gives $N \approx 43$, as one can yield from fig. 7 in paper [5]. Therefore, though not very accurate, the analysis described above may still be useful for obtaining a better estimate of the total number of fluxons.

4.3 Analysis of a Single Fluxon

Although the determination of the fluxon position angles, the angle γ_B, and the scale factor C is a very daunting nonlinear multidimensional parameter estimation problem in the case of many fluxons, this problem can be solved in the case of a single fluxon, $N = 1$. A possible method for obtaining all of the parameters in this scenario is described here.

First, let us compute the scale factor, C. Note that the third odd harmonics amplitudes, D_1 and E_1, may be written by (28) in terms of the first odd harmonics amplitudes, D_0 and E_0.

$$D_1 = 1/3(\cos 3q_+ - \cos 3q_-) = 4/3(\cos q_+ - \cos q_-)^3 + 4\cos q_+ \cos q_-(\cos q_+ - \cos q_-) - (\cos q_+ - \cos q_-) =$$

$$4/3D_0^3 + 4\cos q_+ \cos q_- D_0 - D_0$$

$$E_1 = 1/3(\sin 3q_+ - \sin 3q_-) = -4/3(\sin q_+ - \sin q_-)^3 - 4\sin q_+ \sin q_-(\sin q_+ - \sin q_-) + (\sin q_+ - \sin q_-) =$$

$$-4/3E_0^3 - 4\sin q_+ \sin q_- E_0 + E_0$$

From these and from equations (29) with the noise neglected, we obtain the following expressions for $\cos q_+ \cos q_-$ and $\sin q_+ \sin q_-$:

$$\cos q_+ \cos q_- = \frac{w_1}{4w_0} - \frac{w_0^2}{3C^2} + \frac{1}{4}$$

$$\sin q_+ \sin q_- = -\frac{x_1}{4x_0} - \frac{x_0^2}{3C^2} + \frac{1}{4}$$

The above equations, together with

$$w_0^2 + x_0^2 = C^2(D_0^2 + E_0^2) = C^2(2 - 2\cos q_+ \cos q_- - 2\sin q_+ \sin q_-),$$

allow us to obtain an expression for C in terms of the odd harmonics amplitudes only:

$$C^2 = \frac{w_0^2 + x_0^2}{3(1 - 0.5w_1/w_0 + 0.5x_1/x_0)} \tag{32}$$

Note that the right hand side of (32) is some function of time which, according to our model, should be a constant, so this can also be used as a crosscheck of our approximation.

Now let us assume that the value of the scale factor has been obtained by this method. There are five parameters we would like to estimate: the position angles of the two half-fluxons $(\xi_+, \eta_+, \xi_-, \eta_-)$ and the angle between the body symmetry axis and the normal to the pick-up loop, γ_B. We first recall that $\tan q = b/a$ from eq. (12), which allows us to write

$$\frac{a_+ a_-}{b_+ b_-} = \frac{w_1/w_0 - 4w_0^2/(3C^2) + 1}{-x_1/x_0 - 4x_0^2/(3C^2) + 1},$$

or, in the form that will be more convenient later,

$$0 = (a_+ a_-)(-x_1/x_0 - 4x_0^2/(3C^2) + 1) - (b_+ b_-)(w_1/w_0 - 4w_0^2/(3C^2) + 1) \tag{33}$$

The expressions for $a_\pm$ and $b_\pm$ in (12) may be rewritten as

$$a_\pm = a_{0\pm} + a_{1\pm}\cos\omega_p t + a_{2\pm}\sin\omega_p t, \qquad b_\pm = b_{1\pm}\cos\omega_p t + b_{2\pm}\sin\omega_p t,$$

where the coefficients are constant functions of the parameters we want to estimate, namely:

$$a_{0\pm} = \cos\gamma_B \cos\xi_\pm, \quad a_{1\pm} = \sin\xi_\pm \cos\eta_\pm, \quad a_{2_\pm} = -\sin\xi_\pm \sin\eta_\pm,$$

$$b_{1\pm} = \cos\gamma_B \sin\xi_\pm \sin\eta_\pm, \quad b_{2\pm} = \cos\gamma_B \sin\xi_\pm \cos\eta_\pm.$$

Consequently, the products a_+a_- and b_+b_- may also be written in a similar form, which removes all time-dependence to the trigonometric functions of $\omega_p t$:

$$a_+a_- = a'_0 + a'_1 \cos\omega_p t + a'_2 \sin\omega_p t + a'_3 \cos 2\omega_p t + a'_4 \sin 2\omega_p t$$

$$b_+b_- = b'_0 + b'_1 \cos 2\omega_p t + b'_2 \sin 2\omega_p t,$$

with

$$a'_0 = a_{0+}a_{0-} + (a_{1+}a_{1-} + a_{2+}a_{2-})/2, \quad a'_1 = a_{1+}a_{0-} + a_{1-}a_{0+}, \quad a'_2 = a_{2+}a_{0-} + a_{2-}a_{0+},$$

$$a'_3 = (a_{1+}a_{1-} - a_{2+}a_{2-})/2, \quad a'_4 = (a_{1+}a_{2-} + a_{2+}a_{1-})/2,$$

$$b'_0 = (b_{1+}b_{1-} + b_{2+}b_{2-})/2, \quad b'_1 = (b_{1+}b_{1-} - b_{2+}b_{2-})/2, \quad b'_2 = (b_{1+}b_{2-} + b_{2+}b_{1-})/2.$$

If the expressions for a_+a_- and b_+b_- obtained above are substituted into equation (33), we see that we have an equation of the form

$$\mathcal{Z}(t) = \sum_{j=1}^{j=7} K_j H_j(t) \mathcal{Z}_j(t),$$

where the output signal $\mathcal{Z}$ is given by

$$\mathcal{Z} = w_1/w_0 - 4w_0^2/(3C^2) + 1,$$

$H_j(t)$ are known the polhode harmonics,

$$H_1(t) = 1, \quad H_2(t) = \cos\omega_p t, \quad H_3(t) = \sin\omega_p t,$$

$$H_4(t) = H_6(t) = \cos 2\omega_p t, \quad H_5(t) = H_7(t) = \sin 2\omega_p t,$$

$\mathcal{Z}_j(t)$ are known combinations of the harmonics amplitudes from the GP-B HF telemetry,

$$\mathcal{Z}_1(t) = \mathcal{Z}_2(t) = \mathcal{Z}_3(t) = \mathcal{Z}_4(t) = \mathcal{Z}_5(t) = -x_1/x_0 - 4x_0^2/(3C^2) + 1,$$

$$\mathcal{Z}_6(t) = \mathcal{Z}_7(t) = -w_1/w_0 + 4w_0^2/(3C^2) - 1,$$

and the unknown constants K_j are expressed through the five parameters a'_j and three parameters b'_j,

$$K_1 = \frac{a'_0}{b'_0}, K_2 = \frac{a'_1}{b'_0}, K_3 = \frac{a'_2}{b'_0}, K_4 = \frac{a'_3}{b'_0}, K_5 = \frac{a'_4}{b'_0}, K_7 = \frac{b'_1}{b'_0}, K_8 = \frac{b'_2}{b'_0},$$

which are, in turn, the above combinations of angles we are trying to estimate. Thus we have a linear paramter estimation problem. Various filtering techniques, such as batch filters or Kalman filters, may be used to determine the values of K_j. A second step, consisting of the application of some error minimization technique, will then allow us to obtain the values of the five parameters $\xi_\pm, \eta_\pm$ and γ_B that best fit the overdetermined system of equations relating them to the seven constants K_j.

Although the results of the application of this method were not ready in time to be included in this thesis, a more thorough investigation of it and a further search for other trapped flux analysis methods will continue over the summer.

Acknowledgments

The author is deeply greatful to his adviser, Dr. A. S. Silbergleit, for his time and invaluable assistance throughout this project. The author also thanks Dr. Mac Keiser, Dr. Michael Heifetz, Ilya Nemenman and other members of the GP-B team.

References

[1] F.London, *Superfluids*, vol. 1, Dover, New York, 1961.

[2] A.C.Rose-Innes, E.H.Rhoderick, *Introduction to Superconductivity*, Pergamon Press, Oxford, New York, 1978.

[3] L.L.Wai, *The Effect of Magnetic Trapped Flux Quanta on the London Moment Redout in GP-B*, BS Honors Thesis, Dept. of Physics, Stanford University, 1989.

[4] G.M.Keiser, A.S.Silbergleit, *Pick-up Loop Symmetry and Centering*, Gravity Probe B Document S0243, 1995

[5] I.M.Nemenman, A.S.Silbergleit, *Explicit Green's function of a boundary value problem for a sphere and trapped flux analysis in Gravity Probe B experiment*, Journal of Applied Physics, v.86, n.1, pp.614-624, July 1999.

[6] G.M. Keiser et al., *Gravity Probe B Data Reduction and Simulation Algorithms. End-to-end Test 2: Summary.*, Gravity Probe B Document S0420, 2000.

[7] H.Bateman, A.Erdélyi, *Higher Transcendental Functions*, vol. 2, McGraw-Hill Book Co., New York, Toronto, London, 1953.

[8] H.B.Dwight, *Tables of Integrals and Other Mathematical Data*, fourth edition, The Macmillan Co., New York, 1961.

[9] J.B.Marion, S.T.Thornton, *Classical Dynamics of Particles and Systems*, fourth edition, Hartcourt Brace College Publishing, Fort Worth, 1995.

[10] G.Korn and T.Korn, *Mathematical Handbook for Scientists and Engineers*, McGraw-Hill, New York, 1961.

[11] A.N.Tihonov, A.A.Samarskiy, A.A.Arsen'ev. Russian Journal of Mathematical Physics, 1972.

[12] A.S.Silbergleit, E.A.Tropp, *On the Near Field of Wires, Current-Carrying Plates and Shells*, Soviet Physics: Technical Physics, v. 27, n.2, 1982.